VII International Conference on Adaptive Modeling and Simulation
ADMOS 2015
F. Chinesta, L. Chamoin, P. Díez (Eds)

CONVERGENT ERROR-CONTROLLED MESH ADAPTATION

GAUTIER BRÈTHES*, ADRIEN LOSEILLE†, FRÉDÉRIC ALAUZET† AND ALAIN DERVIEUX*

*INRIA
2004 Route des lucioles, F-06902 Sophia Antipolis
Gautier.Brethes@inria.fr
http://www-sop.inria.fr/members/Gautier.Brethes/Gautier.Brethes.htm
Alain.Dervieux@inria.fr
http://www-sop.inria.fr/members/Alain.Dervieux/Alain_Dervieux-french.html

†INRIA
BP 105, Domaine de Voluceau, F-78153 Le Chesnay
Adrien.Loseille@inria.fr
https://www-roc.inria.fr/gamma/gamma/Membres/CIPD/Adrien.Loseille/index.php
Frederic.Alauzet@inria.fr
https://www-roc.inria.fr/gamma/gamma/Membres/CIPD/Frederic.Alauzet/index.en.html

Key words: Poisson problem, Compressible flow, goal-oriented mesh adaptation, anisotropic mesh adaptation, adjoint, metric

Abstract. In this paper, mesh adaptation is studied as a method for improving mesh convergence and error control. The mesh convergence under study is L^2-norm convergence of the approximation error. The novel mesh-adaptation method tends to minimize this error norm. It somehow extends the goal-oriented formulation since it is equation-based and uses an adjoint. The main novel ingredient is a corrector which evaluates the approximation error. Applications to a Poisson problem and to steady Euler flows are described.

1 INTRODUCTION

Today, the deviation between a continuous PDE solution and its approximation on a given mesh is not sufficiently controlled. Two well-identified processes can help in evaluating this deviation or error. Nested iteration consists in using embedded meshes, measuring the convergence order and possibly comparing it to a theoretical convergence order. Then a Richardson analysis can give a reliable estimate of the error. However, a necessary condition for doing this is that mesh convergence holds with a well-identified order, possibly the theoretical order of the numerical scheme. A systematic procedure to evaluate that

convergence is, for example, convergence grid index method, [12]. The second approach is the use of *a posteriori* error estimates. Generally, these estimates are sufficiently accurate only if a reasonable mesh convergence holds. Then, not only Richardson analysis but also *a posteriori* error estimates need to be combined with a convergent nested iteration. In some cases, these estimates can become correctors and be used for improving the result, see [5] for correctors applying to scalar outputs. Now, the convergence of a nested iteration can be bad due to the -possibly combined- following factors:
(i)- bad initial meshes are used,
(ii)- the rapid increasing of number of unknowns in the nested iteration leads to abandon before convergence,
(iii)- the presence of very different scales and even of singularities in the unknown solution makes the asymptotic convergence out of reach.

In order to get mesh convergence more easily, our research concentrates on anisotropic mesh adaptation. Anisotropic mesh adaptation evidently adresses issues (i) and (iii) but, with the metric parametrisation, it can also adress (ii) by replacing embedded meshes by proportional metrics, a point which shall not be further discussed in the present paper.

Let us discuss what we call a mesh adaptation adequate to the numerical convergence of a prescribed norm of the error. Mainly for the sake of simplicity, we shall restrict to L^2 convergence of the solution field. Our proposal is to minimize the L^2 approximation error norm with respect to a metric-based parametrisation of the mesh.

Since the approximation error is not available, we replace it by what we call an *a posteriori* corrector. Its L^2 norm is our cost functional to minimise. The independant variable for minimisation is the anisotropic metric. Both corrector and metric are defined in our Section 2.

In a Section 3, the novel norm-oriented mesh adaptation is introduced as the result of a generalisation of Hessian-based and of goal-oriented mesh adaptation. In order to minimise the goal-oriented and norm-oriented cost function, we develop for an elliptic problem an *a priori* analysis.

In Section 4, we give a numerical example of the proposed method.

Section 5 is devoted to an extension to the Euler model of Fluid Mechanics.

2 MESH ADAPTATION STATEMENT

2.1 Finer-grid corrector for a generic PDE

We consider a linear PDE denoted $Au = f$ and a second-order accurate discretization of it, $A_h u_h = f_h$. Let us assume the problem is smooth and that the approximation is in its asymptotic mesh convergence phase for the mesh Ω_h under study, of size h. Then, this will be also true for a strictly two-times finer embedding mesh $\Omega_{h/2}$. We would have:

$$u_h = A_h^{-1} f_h \quad , \quad u_{h/2} = A_{h/2}^{-1} f_{h/2} \quad \Rightarrow \quad u - u_{h/2} \approx \frac{1}{4}(u - u_h) \tag{1}$$

where u_h and $u_{h/2}$ are respectively the solutions on Ω_h and $\Omega_{h/2}$. We have also $\Pi_h u - \Pi_h u_{h/2} \approx \frac{1}{4}(\Pi_h u - u_h)$. This motivates the definition of a finer-grid Defect-Correction (DC) corrector as follows:

$$A_h \bar{u}'_{DC} = \frac{4}{3} R_{h/2\to h}(A_{h/2} P_{h\to h/2} u_h - f_{h/2}) \tag{2}$$

where the residual transfer $R_{h/2\to h}$ accumulates, on coarse grid vertices, the values at fine vertices in neighboring coarse elements multiplied with barycentric weights and $P_{h\to h/2}$ linearly interpolates coarse values on fine mesh. In the case of local singularities, statement (1) is not true for uniform meshes but we have some hints that it holds almost everywhere for a sequence of adapted meshes, according to [9]. The DC corrector $\bar{u}'_{DC}$ approximates $\Pi_h u - u_h$ instead of $u - u_h$ and can be corrected as the previous one:

$$u'_{DC} = \bar{u}'_{DC} - (\pi_h u_h - u_h). \tag{3}$$

This field will play a key role in the norm-oriented mesh adaptation introduced in the sequel.

2.2 Mesh parametrization

We propose to work in the continuous mesh framework introduced in [6, 7]. The main idea of this framework is to model discrete meshes by continuous Riemannian metric fields. It allows us to define the adaptation problem as a differentiable optimization problem , *i.e.,* to apply, on the class continuous metrics, a calculus of variations which cannot be applied on the class of discrete meshes. This framework lies in the class of metric-based methods. A continuous mesh $\mathcal{M}$ of the computational domain Ω is identified to a Riemannian metric field [3] $\mathcal{M} = (\mathcal{M}(\mathbf{x}))_{\mathbf{x}\in\Omega}$ where $\mathcal{M}(\mathbf{x})$ is a symmetric 3×3 matrix. We define the *total number of vertices* of $\mathcal{M}$ as:

$$\mathcal{C}(\mathcal{M}) = \int_\Omega \sqrt{\det(\mathcal{M}(\mathbf{x}))}\,\mathrm{d}\mathbf{x}.$$

Given a continuous mesh $\mathcal{M}$, we shall say that a discrete mesh $\mathcal{H}$ of the same domain Ω is a *unit mesh with respect to* $\mathcal{M}$ if each triangle $K \in \mathcal{H}$, defined by its list of edges $(\mathbf{a}_i\mathbf{b}_i)_{i=1\ldots 3}$, verifies:

$$\forall i \in [1,3], \quad \int_0^1 \sqrt{{}^t\mathbf{a}_i\mathbf{b}_i\ \mathcal{M}(\mathbf{a}_i + t\,\mathbf{a}_i\mathbf{b}_i)\ \mathbf{a}_i\mathbf{b}_i}\ \mathrm{d}t \in \left[\frac{1}{\sqrt{2}}, \sqrt{2}\right].$$

The rest of the paper will try to find the best metric $\mathcal{M}$ from various error analyses.

3 THREE OPTIMAL METRICS

3.1 Interpolation-based optimal metric

Let u be any smooth enough function defined on Ω. Let $\mathcal{M}$ be a mesh/metric of Ω. We consider only meshes $\mathcal{M}$ involving enough nodes for justifying the replacement of the

complete error by its main asymptotic part. The P^1 interpolation error $|\Pi_{\mathcal{M}} u - u|$ can be approximated in terms of second derivatives of u and of the metric $\mathcal{M}$ by the *continuous interpolation error:*

$$|\Pi_{\mathcal{M}} u - u| \approx |u - \pi_{\mathcal{M}} u| \text{ with } |u - \pi_{\mathcal{M}} u|(\mathbf{x}) \;=\; \frac{1}{10}\text{trace}(\mathcal{M}^{-\frac{1}{2}}(\mathbf{x})\,|H_u(\mathbf{x})|\,\mathcal{M}^{-\frac{1}{2}}(\mathbf{x})) \quad (4)$$

where $|H_u|$ is deduced from H_u by taking the absolute values of its eigenvalues. Starting from:

$$\|u - \pi_{\mathcal{M}} u\|_{\mathbf{L}^p(\Omega_h)} = \left(\int_\Omega \Big(\text{trace}\big(\mathcal{M}^{-\frac{1}{2}}(\mathbf{x})|H_u(\mathbf{x})|\mathcal{M}^{-\frac{1}{2}}(\mathbf{x})\big)\Big)^p \,\mathrm{d}\mathbf{x}\right)^{\frac{1}{p}}, \quad (5)$$

we define as optimal metric the one which minimizes the right hand side under the constraint of a total number of vertices equal to a parameter N. After solving analytically this optimization problem, we get the unique optimal $(\mathcal{M}_{\mathbf{L}^p}(\mathbf{x}))_{\mathbf{x}\in\Omega}$ as:

$$\mathcal{M}_{\mathbf{L}^p} = \mathcal{K}_p(H_u) = D_{\mathbf{L}^p}\,(\det|H_u|)^{\frac{-1}{2p+2}}\,|H_u| \;\text{ and }\; D_{\mathbf{L}^p} = N\left(\int_\Omega (\det|H_u|)^{\frac{p}{2p+2}}\right)^{-1} \quad (6)$$

where $D_{\mathbf{L}^p}$ is a global normalization term set to obtain a continuous mesh with complexity N and $(\det|H_u|)^{\frac{-1}{2p+2}}$ is a local normalization term accounting for the sensitivity of the $\mathbf{L}^p$ norm. In the case of an adaptation loop for solving a Partial Differential Equation, a continuous function u is not available. Only an approximate solution $u_{\mathcal{M}}$ is available. In that case, the continuous interpolation error (4) is replaced by:

$$|u_{\mathcal{M}} - \pi_{\mathcal{M}} u_{\mathcal{M}}|(\mathbf{x}) \;=\; \frac{1}{10}\text{trace}(\mathcal{M}^{-\frac{1}{2}}(\mathbf{x})\,|H_{u_{\mathcal{M}}}(\mathbf{x})|\,\mathcal{M}^{-\frac{1}{2}}(\mathbf{x})) \quad (7)$$

where $H_{u_{\mathcal{M}}}$ is an approximate Hessian evaluated with the patch-recovery approximation defined in [11]. According to the continuous mesh framework, statement (6) defines directly a continuous optimal metric. In practice, solving (6) is done by approximation, *i.e.* in a discrete context with a couple (mesh, solution) denoted $(\mathcal{H}_{\mathcal{M}}, u_{\mathcal{M}})$ and iteratively through the following fixed point:
Step 1: compute the discrete state $u_{\mathcal{M}}$ on mesh $\mathcal{H}_{\mathcal{M}}$,
Step 2: compute sensor $s_{\mathcal{M}} = s(u_{\mathcal{M}})$ and optimal metric $\mathcal{M}^{opt}_{inter} = \mathcal{K}_p(H_{\mathcal{M}}(s_{\mathcal{M}}))$,
Step 3: $\mathcal{M} = \mathcal{M}^{opt}_{inter}$, generate $\mathcal{H}_{\mathcal{M}} = \mathcal{H}_{\mathcal{M}^{opt}_{inter}}$ and go to 1, until convergence.

The above notation $\mathcal{K}_p$ will also be used in the next sections for $p = 1$.

3.2 Scalar output "goal-oriented" analysis

The goal-oriented analysis relies on the minimization of the error $\delta j_{goal}(\mathcal{M})$ committed on a scalar output $j = (g, u)$, error which we simplify as follows:

$$\delta j_{goal}(\mathcal{M}) = |(g, u - u_{\mathcal{M}})| = |(g, \Pi_{\mathcal{M}} u - u_{\mathcal{M}} + u - \Pi_{\mathcal{M}} u)|. \quad (8)$$

The term $u - \Pi_{\mathcal{M}} u$, similar to the main term of the Hessian-based adaptation in Section 3.1, can be explicitly approached in the same way. The term $\Pi_{\mathcal{M}} u - u_{\mathcal{M}}$ will be transformed via a discrete adjoint state $u^*_{g,\mathcal{M}}$ defined by:

$$\forall \psi_{\mathcal{M}} \in V_{\mathcal{M}}, \quad a(\psi_{\mathcal{M}}, u^*_{g,\mathcal{M}}) = (\psi_{\mathcal{M}}, g). \tag{9}$$

Then:

$$\delta j_{goal}(\mathcal{M}) = |a(\Pi_{\mathcal{M}} u - u_{\mathcal{M}}, u^*_{g,\mathcal{M}}) + (g, u - \Pi_{\mathcal{M}} u)|$$

and, introducing the continuous interpolation error (7), we get:

$$\delta j_{goal}(\mathcal{M}) \preceq |a(\Pi_{\mathcal{M}} u - u_{\mathcal{M}}, u^*_{g,\mathcal{M}})| + |g||\pi_{\mathcal{M}} u_{\mathcal{M}} - u_{\mathcal{M}}|.$$

The first variational term can be estimated as in [1]:

$$\delta j_{goal}(\mathcal{M}) \ \preceq \ \int_\Omega \left(\ [\frac{1}{\rho} \bar{\rho}(H(u^*_{g,\mathcal{M}})) + |g|] \ |\pi_{\mathcal{M}} u_{\mathcal{M}} - u_{\mathcal{M}}| \ + \ |u^*_{g,\mathcal{M}}| \ |\pi_{\mathcal{M}} f - f| \ \right) \ \mathrm{d}\Omega$$

where we have introduced the discrete extension of the interpolation error. It is then reasonable to try to minimize the RHS of this inequality instead of the LHS. However, this still involves some difficulty due to the dependancy of adjoint state $u^*_{g,\mathcal{M}}$ with respect to $\mathcal{M}$. We shall further simplify our functional by freezing, during a part of the algorithm, the adjoint state. The idea is that, when we change the parameter $\mathcal{M}$, $u^*_{g,\mathcal{M}}$ is close to its (non-zero) continuous limit and is not much affected, in contrast to the interpolation errors $|\pi_{\mathcal{M}} u_{\mathcal{M}} - u_{\mathcal{M}}|$ and $|\pi_{\mathcal{M}} f - f|$. We then consider, for a given $\mathcal{M}_0$, the following optimum problem:

$$\min_{\mathcal{M}} \int_\Omega \left(\ [\frac{1}{\rho} \bar{\rho}(H(u^*_{g,\mathcal{M}_0})) + |g|] \ |\pi_{\mathcal{M}} u_{\mathcal{M}} - u_{\mathcal{M}}| \ + \ |u^*_{g,\mathcal{M}_0}| \ |\pi_{\mathcal{M}} f - f| \ \right) \ \mathrm{d}\Omega.$$

This will produce an optimum:

$$\mathcal{M}_{opt,\mathcal{M}_0} = \arg\min_{\mathcal{M}} |tr(\mathcal{M}^{-1/2} \left([\frac{1}{\rho} \bar{\rho} H(u^*_{g,\mathcal{M}_0}) + |g|] |H_u| + |u^*_{g,\mathcal{M}_0}||H_f| \right) \mathcal{M}^{-1/2})|.$$

Observing that, in the integrand,

$$H_{goal,0} = [\frac{1}{\rho} \bar{\rho}(H(u^*_{g,\mathcal{M}_0})) + |g|] \ |H_u| \ + \ |u^*_{g,\mathcal{M}_0}| \ |H_f|$$

is a positive symmetric matrix, we can apply the above calculus of variation and get:

$$\mathcal{M}_{opt,\mathcal{M}_0} = \mathcal{K}_1(\ [\frac{1}{\rho} \bar{\rho}(H(u^*_{g,\mathcal{M}_0})) + |g|] \ |H_u| \ + \ |u^*_{g,\mathcal{M}_0}| \ |H_f|).$$

This solution can then be introduced in a fixed-point loop and will produce:

$$\mathcal{M}_{opt,goal} = \mathcal{K}_1(\, [\frac{1}{\rho}\bar{\rho}(H(u^*_{g,\mathcal{M}_{opt,goal}})) + |g|] \, |H_u| \; + \; |u^*_{g,\mathcal{M}_{opt,goal}}| \, |H_f|).$$

Let us precise how the discrete algorithm is organised:
Step 1: compute the discrete state $u_{\mathcal{M}}$ on mesh $\mathcal{H}_{\mathcal{M}}$,
Step 2: compute the discrete adjoint state $W^*_{\mathcal{M}}$,
Step 3: compute optimal metric $\mathcal{M}_{opt,\mathcal{M}}$,
Step 4: $\mathcal{M} = \mathcal{M}_{opt,\mathcal{M}}$, generate $\mathcal{H}_{\mathcal{M}}$ and go to 1, until convergence.

The adaptation of this process to the Euler model of Gas Dynamics is studied in [8] for the steady case and in [2] for the unsteady case.

3.3 Norm-based functional

We are now interested by the minimization of $\delta j(\mathcal{M}) = ||u - u_{\mathcal{M}}||^2_{L^2(\Omega)}$ with respect to the mesh $\mathcal{M}$. Introducing u'_{DC} from (3) gives:

$$\delta j(\mathcal{M}) \approx (u'_{DC}, u - u_{\mathcal{M}}). \tag{10}$$

Let us define the discrete adjoint state $u^*_{\mathcal{M}}$:

$$\forall \psi \in \; V_{\mathcal{M}}, \quad a(\psi_{\mathcal{M}}, u^*_{\mathcal{M}}) = (\psi_{\mathcal{M}}, u'_{DC}). \tag{11}$$

Then, similarly to Section 3.2, we have to solve the following optimum problem.

$$\min_{\mathcal{M}} \int_\Omega \left(\; [\frac{1}{\rho}\bar{\rho}(H(u^*_{\mathcal{M}})) + |u'_{DC}|] \; |\pi_{\mathcal{M}} u_{\mathcal{M}} - u_{\mathcal{M}}| \; + \; |u^*_{\mathcal{M}}| \, |\pi_{\mathcal{M}} f - f| \; \right) \, \mathrm{d}\Omega.$$

Exactly as for Section 3.2, we freeze the dependancy of the adjoint state.

$$\min_{\mathcal{M}} \int_\Omega \left(\; [\frac{1}{\rho}\bar{\rho}(H(u^*_{\mathcal{M}_0})) + |u'_{DC}|] \; |\pi_{\mathcal{M}} u_{\mathcal{M}} - u_{\mathcal{M}}| \; + \; |u^*_{\mathcal{M}_0}| \, |\pi_{\mathcal{M}} f - f| \; \right) \, \mathrm{d}\Omega.$$

$$\mathcal{M}_{opt,\mathcal{M}_0} = \mathcal{K}_1(\, [\frac{1}{\rho}\bar{\rho}(H(u^*_{\mathcal{M}_0})) + |u'_{DC}|] \, |H_u| \; + \; |u^*_{\mathcal{M}_0}| \, |H_f|).$$

In order to get the final norm-oriented optimum $\mathcal{M}_{opt,norm}$, we apply:

Step 1: first solve the linearised corrector system (3) in order to get u'_{DC},

Step 2: then, solve the adjoint system:

$$a(\psi, u^*_{DC,\mathcal{M}}) = (u'_{DC}, \psi) \tag{12}$$

Step 3: finally, put:

$$\mathcal{M}^{(\alpha+1)} = \mathcal{K}_1([|u'_{DC}| + \frac{1}{\rho}\bar{\rho}H(u^*_{prio})] \, |H_{u_{\mathcal{M}}}| + |u^*_{prio}||H_f|) \tag{13}$$

the three-step process being re-iterated until we get a fixed point $\mathcal{M}_{opt,norm} = \mathcal{M}^{(\infty)}$.

4 APPLICATION TO A POISSON PROBLEM

We restrict our study to an example from a benchmark of two-dimensional Poisson problems, cf. [4]. We conjecture that the two following mesh adaptation methods produce L^2 convergent solutions to continuous. The first method, the Hessian-based method (with $p = 2$), is just heuristically relying on usual finite-element estimates. The second method, our novel norm-oriented method, is directly built on the minimisation of the L^2 error norm. We do not consider goal-oriented applications for which examples of computations can be found in [8] and [2].

4.1 Numerical features

In [4], a mesh-adaptative full-multigrid (FMG) algorithm relying on the Hessian-based adaptation criterion is designed. We first describe in short this algorithm for the Hessian-based option. A sequence of numbers N_k of vertices is specified from a coarse mesh to finer one $N_0 = N, N_1 = 4N, N_2 = 16N, N_3 = 64N, ...$ For each mesh size N_k, a sequence of adapted meshes of size N_k is built by iterating the following loop:
(1) computing a solution,
(2) computing the optimal metric,
(3) building the adapted mesh.
In (1), a multi-grid V-cycle is applied to a sufficient convergence. In (2), approximations of the Hessians are performed as in [8]. When changing of mesh, an interpolation is applied in order to enjoy a good initial condition. About 4 adaptation iterations are applied at each mesh fineness N_k.

The extension of the above loop to norm-oriented adaptation consists in replacing the single Hessian evaluation by:
- the computation of the corrector, using MG and the best available (interpolated to current mesh) previous evaluation,
- the computation of the adjoint, using MG and also the best available (interpolated to current mesh) previous evaluation,
- the evaluation of (13).

4.2 Bubble-like test case with thick interface

We are interested by the Poisson problem solution u which is equal to 1 on a disk and to 0 in the rest of the domain. This function is the prototype of the pressure in a multi-fluid flow involving capillary forces. The source term is a Dirac derivative. We smoothen this computation by defining a thickness ε of an annular region separing the two subdomains (outside the disk, inside the disk) and in which u is smoothly varying from 0 to 1 as shown in figure 1. If (x, y) is located inside the annular region, $u(x, y)$ is given by the formula: $u(x, y) = \frac{1}{2} + \frac{1}{2} sin(\frac{\pi\psi}{\varepsilon})$ with $\psi = 0.25 - \sqrt{(x_C - x)^2 + (y_C - y)^2}$. From this solution, a right-hand side f is computed. Given a mesh, vertex values of f_h are interlopated from the analytic f. As a result, for rather coarse meshes, the zone where f is not zero can be

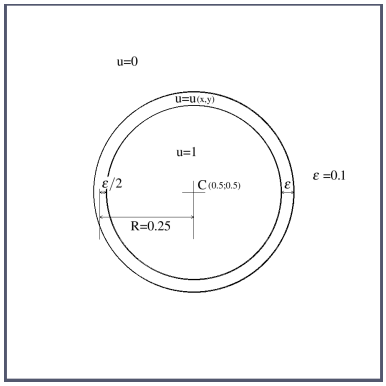

Figure 1: Circular-test-case-domain: sketch of the solution u.

simply missed and f_h can be zero even in the neighborhood of the high values of f. We consider a thickness of $\varepsilon = 0.1$.

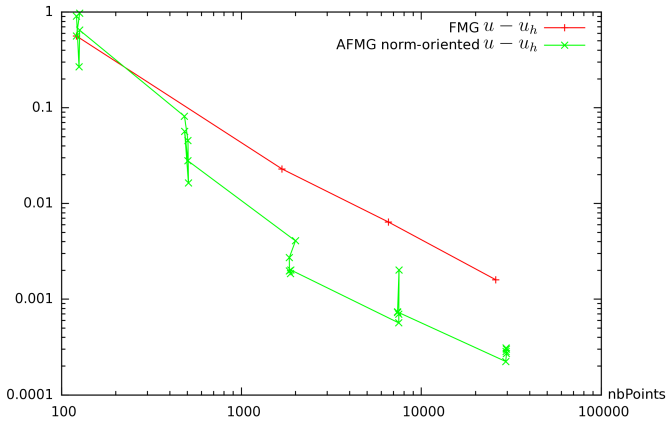

Figure 2: Thick bubble test case: convergence of the error norm $|u - u_h|_{L^2}$ as a function of number of vertices in the mesh for (+) non-adaptative FMG, (×) Hessian-based adaptative FMG and (∗) norm-oriented adaptative FMG.

Two methods are compared in Figure 2: standard FMG with a sequence of uniform meshes and norm-oriented adaptative FMG. The proposed norm-oriented adaptative method behaves in a better way with a five times smaller error than for the uniform refinement.

In practical applications, an analytic solution is of course not available. We have then two possible measures of the convergence. The standard method consists in comparing the solutions on successive meshes and apply a convergence analysis as in [12]. We can also use our corrector as a prediction of the approximation error. Fig. 3 compares the norm of the actual error with the norm of the corrector. We observe a very similar behavior

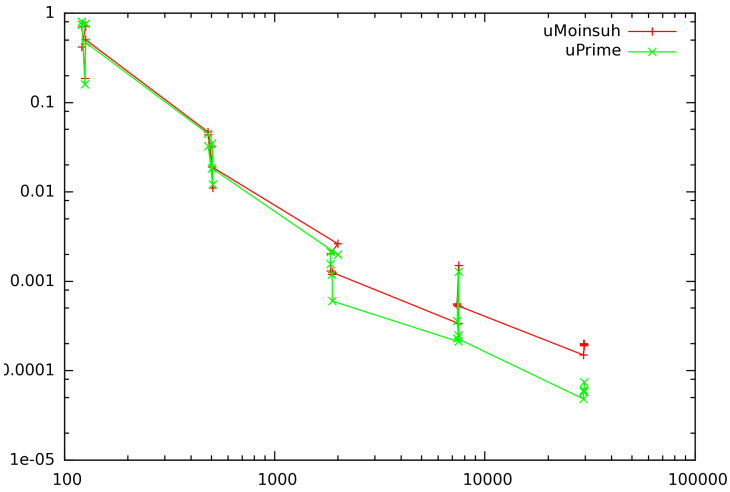

Figure 3: Thick bubble test case: convergence of the error norm $|u-u_h|_{L^2}$ compared to the convergence of the corrector norm $|u'_h|_{L^2}$.

but a correction factor of about 7 has to be applied, like:

$$|u - u_h| \approx 7|u'_h|$$

in order to get a better prediction. However, this factor probably depends on the smoothness of the solution and degrades with mesh convergence.

5 APPLICATION TO EULER FLOW

5.1 Methods

The above norm-oriented mesh adaptation has been extended to Euler flow adaptation. Let us denote $\Psi(W) = 0$ the steady Euler equations where $W = \{\rho, \rho\mathbf{u}, \rho E\}$ is the set of conservation variables. Let $\Psi_h(W_h) = 0$ be its discretization by a vertex-centered second-order upwind scheme. The DC evaluation of the corrector writes:

$$\frac{\partial \Psi_h}{\partial W}\bar{W}'_{DC} = \frac{4}{3}R_{h/2\to h}\Psi_{h/2}(P_{h\to h/2}W_h), \quad W'_{DC} = \bar{W}'_{DC} - (\pi_h W_h - W_h). \tag{14}$$

Then

$$\frac{\partial \Psi_h}{\partial W} g'_{DC} = W'_{DC}. \tag{15}$$

In practice, a nonlinear version of (15) is used. The rest of the algorithm is very similar to a goal-oriented algorithm for which we follow the lines of [8].

5.2 An example

We consider the geometry provided for the 1st AIAA CFD High Lift Prediction Workshop (Configuration 1). We consider an inflow at Mach 0.2 with an angle of attack of 13

degrees. Three adaptation strategies are compared. The first one controls the interpolation error on the density, velocity and pressure in L^1 norm. The second one controls the interpolation error on the Mach number. The third one is based on the norm-oriented approach and controls the norm of the approximation error $||W - Wh||_{L^2}$. For each case, five adaptations at fixed complexity are performed for a total of 15 adaptations with the following complexities: [160 000, 320 000, 640 000]. This choice leads to final meshes having around 1 million vertices. The residual for the flow solver convergence is set to 10^{-9} for each case. The generation of the anisotropic meshes is done with the local remeshing strategy of [10]. The surface meshes and the velocity iso-lines are depicted in Figure 4. Depending on the adaptation strategy, completely different flow fields are observed. The adaptation on the Mach number reveals strong shear layers at the wing tip that are not present in the norm-oriented approach. On the contrary, recirculating flows are observed on the norm-oriented approach while not being observed on the Mach number adaptation. For each case, the wakes have different features. Note that the accuracy near the body is not equivalent. For the L^1 norm adaptation error and norm-oriented approaches, the far-field and inflow are much more refined than in the Mach number adaptation. This leads to unresolved phenomena for the final considered complexity. This example illustrates the need to control the whole flow field. Indeed, if the adaptation on the Mach number can provide a second-order convergent field, there is no guarantee on the other fields (density, pressure, velocity,...). In addition, the adaptation with the norm-oriented approach tends to increase the refinement also at the inflow boundary condition and also at the far-field although the interpolation error (on all variables) is negligible in these areas. Consequently, it seems of main interest to control all the sources of error, especially when the final intent is to certify a flow simulation.

6 CONCLUSION

The norm-oriented mesh adaptation method is an answer to a well-formulated problem: we choose an error norm and prescribe a number of nodes and we have to find the mesh giving the smallest approximation error in that norm. The norm-oriented mesh adaptation method transforms the problem into an optimization problem which is mathematically well-posed. For this, a Defect-Correction corrector is built from a finer-mesh defect correction principle. The norm-oriented method is presented as a natural extension of the goal-oriented method which, in our formulation, is itself a natural extension of the Hessian-based method. More precisely, while the Hessian-based method solves only the PDE under study, the goal-oriented method also solves an adjoint system (with linearised operator, transposed). The norm-oriented solves three systems, a corrector (linearised system with an adhoc RHS), an adjoint (linearised and transposed, with the corrector as RHS) and the PDE itself. The three algorithms have in common an anisotropic *a priori* error analysis and a metric-based mesh parametrisation. The Hessian-based method produces convergent solution fields but does not take into account the precise equation and discretization. The goal-oriented method takes into account equation and discretization

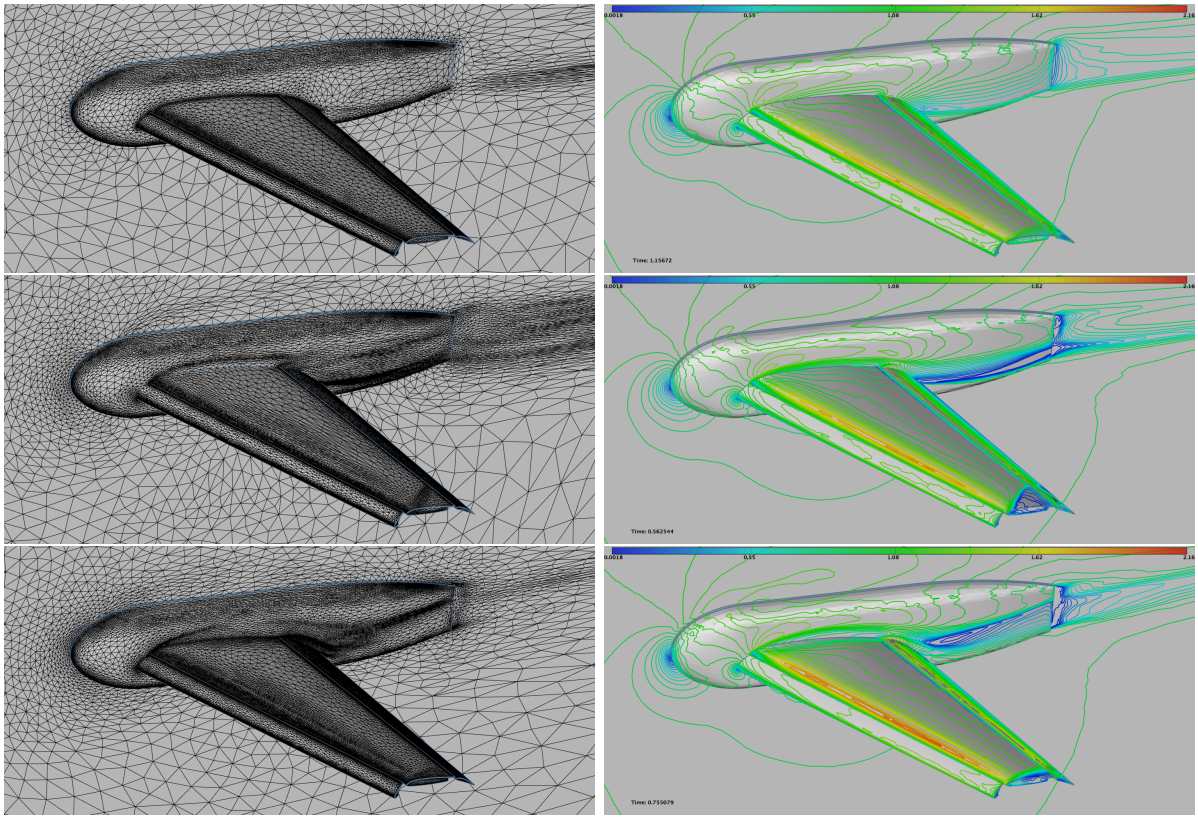

Figure 4: Surface mesh and velocity iso-values when controlling the sum of the L^1 norm of the interpolation error on the density, velocity and pressure (top), the Mach number (middle) and the norm $||W - Wh||_{L^2}$ with the norm-oriented approach (bottom).

but is too focused on a particular output and does not produce convergent solution fields. The norm-oriented method has the advantages of both. For elliptic problems, the Hessian-based approach is nearly optimal as suggested by finite-element estimates. However, the presented comparisons seem to indicate that the novel method carries a good improvement. We have also proposed a preliminary application to an inviscid compressible flow. New computations will be shown during the conference.

7 ACKNOWLEDGEMENTS

This work has been supported by French National Research Agency (ANR) through project MAIDESC n^o ANR-13-MONU-0010. This work was partly done in the UMRIDA project which is supported by the European Commission under contract No. ACP3-GA-2013-605036. The first author is supported by region PACA and Lemma Engineering company.

REFERENCES

[1] A. Belme. *Aérodynamique instationnaire et méthode adjointe*. PhD thesis, Université de Nice Sophia Antipolis, Sophia Antipolis, France, 2011. (in French).

[2] A. Belme, A. Dervieux, and F. Alauzet. Time accurate anisotropic goal-oriented mesh adaptation for unsteady flows. *J. Comp. Phys.*, 231(19):6323–6348, 2012.

[3] M. Berger. *A panoramic view of Riemannian geometry*. Springer Verlag, Berlin, 2003.

[4] G. Brèthes, O. Allain, and A. Dervieux. A mesh-adaptive metric-based Full-Multigrid for the Poisson problem. *submitted to I.J. Numer. Meth. Fluids*, 2014.

[5] M.B. Giles and N.A. Pierce. *Adjoint Error Correction for Integral Outputs*, volume 25 of *Lecture Notes in Computational Science and Engineering, editors T. Barth and H. Deconinck*, pages 47–96. Springer-Verlag, 2002.

[6] A. Loseille and F. Alauzet. Continuous mesh framework. Part I: well-posed continuous interpolation error. *SIAM Journal on Numerical Analysis*, 49(1):38–60, 2011.

[7] A. Loseille and F. Alauzet. Continuous mesh framework. Part II: validations and applications. *SIAM Journal on Numerical Analysis*, 49(1):61–86, 2011.

[8] A. Loseille, A. Dervieux, and F. Alauzet. Fully anisotropic goal-oriented mesh adaptation for 3D steady Euler equations. *J. Comp. Phys.*, 229(8):2866–2897, 2010.

[9] A. Loseille, A. Dervieux, P.J. Frey, and F. Alauzet. Achievement of global second-order mesh convergence for discontinuous flows with adapted unstructured meshes. In *37th AIAA Fluid Dynamics Conference and Exhibit*, AIAA-2007-4186, Miami, FL, USA, Jun 2007.

[10] A. Loseille and V. Menier. Serial and parallel mesh modification through a unique cavity-based primitive. In J. Sarrate and M. Staten, editors, *Proceedings of the 22th International Meshing Roundtable*, pages 541–558. Springer, 2013.

[11] F. Magoules. *Computational Fluid Dynamics*. CRC Press, Boca Raton, London, New York, Washington D.C., 2011.

[12] P.J. Roache. Perspective: a method for uniform reporting of grid refinement studies. *Journal of Fluid Engineering*, 116:3:405–413, 1994.